



# Characterization of sodium dodecyl sulfate modified iron pillared montmorillonite and its application for the removal of aqueous Cu(II) and Co(II)

Shu-Zhen Li<sup>a</sup>, Ping-Xiao Wu<sup>a,b,\*</sup>

<sup>a</sup> College of Environmental Science and Engineering, South China University of Technology, Guangzhou, 510006, PR China

<sup>b</sup> The Key Lab of Pollution Control and Ecosystem Restoration in Industry Clusters, Ministry of Education, Guangzhou, 510006, PR China

## ARTICLE INFO

### Article history:

Received 6 February 2009

Received in revised form 11 August 2009

Accepted 12 August 2009

Available online 19 August 2009

### Keywords:

Polymers

X-ray photo-emission spectroscopy (XPS)

Microporous materials

Adsorption

## ABSTRACT

Anionic surfactant modified Fe-pillared montmorillonites were prepared by Fe-hydrate solution and sodium dodecyl sulfate (SDS) solution. These organo-inorgano complex montmorillonites were divided into three types (CM1, CM2 and CM3) depending on different intercalation processes. X-ray diffraction spectra, the Fourier transform infrared (FTIR) spectra were used to analyze the structure of the raw and modified montmorillonites. X-ray photoelectron spectra of the samples have been studied to determine spectral characteristics to allow the identification of Fe(III) hydroxide. The specific surface area of the host montmorillonite (M0) is 73.2 m<sup>2</sup>/g, while for the modified montmorillonites it is 114.0 m<sup>2</sup>/g, 117.2 m<sup>2</sup>/g, and 115.8 m<sup>2</sup>/g, respectively. The mesopore volumes of the montmorillonites decrease after modification. Ions of copper and cobalt were selected as adsorbates to evaluate the adsorption performance of each montmorillonite. The adsorption data was analyzed by both Freundlich and Langmuir isotherm models and the data was well fit by the Langmuir isotherm model. The adsorption was efficient and significantly influenced by metal speciation, metal concentration, contact time, and pH. Higher adsorption capacity of the modified montmorillonites were obtained at pH 5–6. The results of desorption indicated that the metal ions were covalently bound to the modified montmorillonites.

© 2009 Elsevier B.V. All rights reserved.

## 1. Introduction

Montmorillonites have been widely used to remove toxic metal ions and organic compounds [1–4]. These clays are useful because of their high specific surface area, chemical and physical stability, and surface structural properties. Many researchers have focused on the surface modifications. They used organic cations to alter the surface properties of clays and improve their adsorption capacity [5,6]. After modification, the characteristics of the clay are remarkably improved, especially the adsorption of organic contaminants [7]. The modification reactions are accomplished by replacing interlayer cations (e.g. Na<sup>+</sup>, K<sup>+</sup>, Ca<sup>2+</sup>) with specific species. There are two main methods of pillaring. The earliest method is inorganic pillaring, using polyhydroxocations such as Al, Fe, Fe–Al, Zr–Fe pillared clays [8–16]. This method has been improved to synthesize clay-based Fe nanocomposite, which is used in the photo-catalytic activity and adsorption [17–19]. Iron-doped pillared clays performed well in the removal of H<sub>2</sub>S from wet air streams, which was

due to the homogenous micropore structure and the high dispersion of catalytically-active metal [20]. The synthesis of organo-clays has focused on intercalation of long-chain quaternary ammonium cations in the interlayer space. The reagents can be alkylammonium derivatives, natural organic cations like L-carnitine, L-cystine dimethyl ester, thiamine, 4-phenylazoaniline, and so on [21–25].

Organo-inorgano complex montmorillonites developed in the last decade are still an active research interest. Plenty of results published on the different adsorbate–adsorbent interactions have confirmed their high efficiency in adsorption of different micropollutants [26–29]. The organic modifiers can change the surface properties of the clays from hydrophilic to hydrophobic, which significantly enhance their affinity for organic contaminants [30]. Alternatively, metal ions can be easily adsorbed with the original hydrophilic clay. Amorphous dense cluster structures in Fe pillared clays are advantageous for adsorption. Polymeric Fe species are the most effective coagulants or adsorption reagents for removing various impurities in potable water treatment [31,32]. A complex of surfactant and polymeric ferric species should have great potential adsorption capacity of different micropollutants. Similar experiments have been conducted by researchers, e.g. Wu synthesized complex modified montmorillonites as adsorbents of phenols [33]; Jiang and Zeng used

\* Corresponding author at: College of Environmental Science and Engineering, South China University of Technology, Guangzhou, 510006, PR China.

E-mail address: [pppxwu@scut.edu.cn](mailto:pppxwu@scut.edu.cn) (P.-X. Wu).

polymeric Fe–Al–hexadecyl–trimethyl–ammonium pillared montmorillonites to adsorb Cu(II) and phenols [34].

The rapid increase in the use of heavy metals over the past few decades has inevitably resulted in an increased flux of metallic substances into the environment. Under favorable pH and other conditions, metals become soluble in water. Metals, pesticides and PCBs have the greatest potential for bioaccumulation [35]. The accumulation of heavy metals in vegetables, fish, grain, and drinking water is of increasing concern in China, as it relates to food safety, potential health risks and ecological damage, especially in industrial districts [36–38]. Huang suggested paying more attention to the potential threat of heavy metals to the health of rural inhabitants through consumption of wheat in Kunshan, China [39]. Heavy metals, such as As, Hg and Cd, have been widely investigated, whereas the research on Cu(II) and Co(II) is inadequate. Co(II) affects the respiratory system, kidneys, and gastrointestinal tract, and Co(II) dermatitis and sensitization as a result of dermal exposure have been well documented by the U.S. Department of Health and Human Services. Gastrointestinal distress is one of the reported health effects of Cu(II), accompanied with vomiting, nausea and abdominal pain as common symptoms of Cu(II) poisoning. Thus, there is a need to search for appropriate ways to protect the environment from pollution by these heavy metals.

This paper reports methods to synthesize an organo-inorgano complex montmorillonite, by improving the process of Fe-pillared montmorillonite. With different surface properties, the changes in the structures and the adsorption of Cu(II) and Co(II) are noted. Based on the results of these characteristics, the quantitative description of adsorption processes through adsorption isotherms and the individual adsorption behavior of Cu(II) and Co(II) are determined. These materials are useful in the restoration of soil and groundwater and as an antidote for ruminants suffering from metal contamination.

## 2. Material and methods

### 2.1. Starting materials and techniques

Montmorillonite, purchased from Nanhai, Guangdong province; had a cation exchange capacity of 78.3 mmol/100 g clay. All of the reagents used in this study were of analytical grade and were purchased from Guangzhou chemical reagent factory (Guangdong Province, China).

Powder X-ray diffraction (XRD) patterns of the montmorillonites in this study were obtained with a Rigaku X-ray diffractometer type D/max-III A at 40 kV and 20 mA with Cu K $\alpha$  radiation with a scan time of 1.0 min<sup>-1</sup>, scanning from 1–40 2 $\theta$  range. Before the XRD test, the samples were dried at 60 °C for 10 h, and pulverized to pass through a 200  $\mu$ m mesh sieve.

Fourier transform infrared (FTIR) spectra of the adsorbents were taken with a Fourier FTIR spectrometer (American Thermo-electron Corporation). The measurement was carried out by using the KBr pellets/disks method. The concentration of the sample in KBr is in the range of 0.2% to 1%. The sample is mixed and ground to a fine powder. The KBr pellets were prepared by using a hydraulic press at a pressure of 20,000 prf. to get a homogenous and transparent appearance.

N<sub>2</sub>-adsorption isotherms were measured using the ASAP 2020 volumetric adsorption analyzer (Micromeritics Instrument Corporation) after degassing the samples under vacuum for 8 h at 423 K. The samples are the same powder used in the XRD measurement. The measurement used the volumetric method. This method uses pure nitrogen instead of a gas mixture of nitrogen and helium, so interfering effects of thermal diffusion can be avoided. The surface areas were calculated using the BET equation. The pore size

distributions were derived from the adsorption branches of the isotherms using the BJH method.

The X-ray photoelectron spectra were measured with an ANELVA AES-430S X-ray photoelectron spectrometer and the binding energy of C 1s was shifted to 284.6 eV as an internal reference. The powder was prepared by the same process as XRD. The powder was sprinkled onto the surface of sticky carbon tape for analysis. The pass energy was 50 eV and a conventional Al K $\alpha$  (1486.7 eV) anode radiation source was used as the excitation source.

The concentrations of Cu(II) and Co(II) were determined by atomic absorption spectrophotometer Z-2000 (Hitachi Zeeman).

#### 2.1.1. Fe-hydroxypolycation solution

For preparation of Fe hydroxypolycation solutions, 3.2 g of sodium carbonate was added slowly as a powder into a 200 mL of 0.1 M solution of iron nitrate under 2 h of constant stirring to achieve a Fe/Na<sub>2</sub>CO<sub>3</sub> molar ratio of 1:5. The solution was aged at 333 K for 24 h. The preparation method was described in [17,40], and the Fe/Na<sub>2</sub>CO<sub>3</sub> molar ratio and the Fe/montmorillonite ratio were changed. Sodium dodecyl sulfate (SDS) was used as the organic reagent instead of Cetyltrimethyl Ammonium Bromide.

#### 2.1.2. Sodium dodecyl sulfate (SDS) solution

Ten g/L sodium dodecyl sulfate (SDS) solution was prepared by dissolution of SDS in distilled water. The purity of SDS was  $\geq$ 99% and was used without further purification.

#### 2.1.3. Preparation of Fe hydroxyl pillared montmorillonite

Four g dry montmorillonite was added to 200 mL distilled water to get 2% (mass) montmorillonite suspension, and then mixed with Fe-hydroxypolycation solution to obtain a Fe/montmorillonite ratio equal to 10 mmol/g under vigorous stirring for 1 h. The resulting solution was aged for 24 h, and then separated by centrifugation, washed several times with distilled water, dried at 60 °C, and pulverized to pass through a 200  $\mu$ m mesh sieve.

#### 2.1.4. Preparation of organic pillared montmorillonite (SDS-M)

Sodium dodecyl sulfate (SDS) solution was added to 2% montmorillonite suspension until the SDS/montmorillonite ratio was 0.6 mmol/g, with vigorous stirring for 2 h, and then separated by centrifugation, washed several times with distilled water, dried at 60 °C, and pulverized to pass through a 200  $\mu$ m mesh sieve.

### 2.2. Preparation of organo-inorgano complex montmorillonites

Three different preparation methods were used:

- (1) CM1: SDS solution was added into 2% Fe hydroxyl pillared montmorillonite suspension until the SDS/montmorillonite ratio was 0.6 mmol/g, with vigorous stirring for 2 h.
- (2) CM2: Four g dried SDS-M was added into distilled water to get 2% (mass) suspension, and then mixed with Fe-hydroxypolycation solution under vigorous stirring for 1 h in order to obtain a Fe/montmorillonite ratio equal to 10 mmol/g. The resulting solution was aged for 24 h.
- (3) CM3 was prepared by adding Fe pillared solution and SDS solution simultaneously into 2% montmorillonite suspension under vigorous stirring for 2 h. The Fe/clay ratio and SDS/clay ratio are 10 mmol/g and 0.6 mmol/g, respectively. In each case, the solution was added drop by drop at ambient temperature. The solid was separated by centrifugation, washed several times with distilled water until free of nitrate or surfactant, dried at 60 °C, and pulverized to pass through a 200  $\mu$ m mesh sieve.

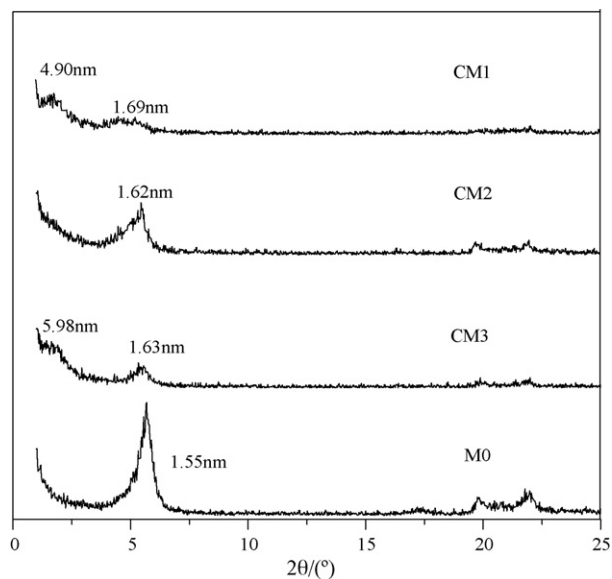


Fig. 1. X-ray patterns of host montmorillonite (M0) and complex modified montmorillonite (CM1, CM2, and CM3).

### 2.3. Adsorption–desorption experiment

The Cu(II) and Co(II) adsorption experiments were conducted by dissolving appropriate amounts of  $\text{CuCl}_2 \cdot 2\text{H}_2\text{O}$  and  $\text{CoCl}_2 \cdot 6\text{H}_2\text{O}$  separately, in distilled water. The pH of Cu(II) and Co(II) solutions were adjusted to 5.0 by addition of 0.01 mol/L HCl or NaOH solution. Batch adsorption experiments were carried out in 150 mL Erlenmeyer flasks by mixing together 0.15 g of adsorbent with 50 mL aqueous solution of metal ions. The flasks were agitated by a table concentrator, and constant temperature maintained with the water bath for a known time interval. The mixture was then centrifuged and the concentration of unadsorbed metal ions remaining in the supernatant liquid was determined by atomic absorption spectrometry.

The desorption experiment was conducted using the following procedure: After adsorption of metal ions, the suspension was centrifuged, and the solid material was mixed with 50 mL distilled water in a 150 mL Erlenmeyer flask and agitated by placing in a water bath thermostat (needs defined) for 24 h. The final suspension was centrifuged again and the concentration of metal ions in the supernatant liquid was determined by atomic absorption spectrometry.

The equilibrium adsorption quantity  $q$  (mg/g) was calculated as:

$$q = \frac{V(C_0 - C)}{1000m}, \quad (1)$$

where  $V$  (mL) is the volume of metal ions in solution,  $m$  (g) is the mass of adsorbent;  $C_0$  and  $C$  ( $\text{mg L}^{-1}$ ) are the concentrations before and after adsorption, respectively.

## 3. Results and discussion

### 3.1. Structural characteristics

#### 3.1.1. X-ray diffraction and FTIR spectra of montmorillonites

The XRD results of montmorillonite and complex modified montmorillonite are shown at Fig. 1. CM1 and CM3 show two reflections. The first unusual one corresponds to large d-spacing and the second to a d-spacing attributed to the (001) reflection. The (001) reflection of M0 is 1.55 nm, which represents a kind of Ca-montmorillonite (Ca-Mt). It has been demonstrated that Ca-Mt also exhibits two d-spacings, and the first XRD peak

with large d-spacing of Ca-Mt has significantly lower intensity than Na-montmorillonite [41]. So it is difficult to detect the first weak and broad peak of M0. Another reason is that some authors reported a raw Ca-Mt sample from Hebei province (China) shows a XRD pattern without the peak at the large d-spacing [41]. This may be true of Ca-Mt used in our experiments. The same authors also concluded that the water treatment process might have had a prominent influence on the porous structure of powdered Mt. The exhibition of large d-spacings of CM2 and CM3 indicates the formation of a secondary house-of-cards structure, which results from the three-dimensional co-aggregation of clay platelets and iron hydroxycations or iron oxides nanoparticles. The disordered porous structure in raw montmorillonites might just be the “house of cards” structure resulting from aggregation of clay platelets [42]. Previous researches have demonstrated that the large d-spacing does not correspond to the classic periodic pillared structure of iron species intercalated into the host montmorillonite but corresponds to a disordered porous structure existed even in the host montmorillonites [41].

The basal spacing of modified montmorillonite was increased slightly by 0.06 nm, indicating that not all the sheets have been intercalated [43], and because Fe-oxycations likely differ in size and are able to interact with clay layers (aggregation and adsorption on the surface of flakes). As indicated in the literature, iron species, besides locating between layers in different forms, can be adsorbed on the outer surfaces of the clay flakes [20]. The 001 reflection of the host clay was sharper and a higher order harmonics appeared, while CM1 and CM3 were dispersed and the intensity was weakened after modification. This suggests the formation of a much more disordered pillared structure. Therefore, the resulting Fe modified montmorillonite show a delaminated structure containing intercalated or pillared fragments. But this reduction did not obviously occur in CM2, and is due to the fact that polycations in the presence of surfactants are protected from hydrolysis resulting in the crystal structure of CM2 being retained.

Fig. 2 shows FTIR spectra of host montmorillonite and modified montmorillonites. The frequencies and assignment of the vibration modes observed are listed in Table 1. The host montmorillonite exhibited bands at  $3434 \text{ cm}^{-1}$  (OH stretching),  $1643 \text{ cm}^{-1}$ ,  $1086 \text{ cm}^{-1}$  (OH bending), and  $695 \text{ cm}^{-1}$ ,  $625 \text{ cm}^{-1}$ , and  $519 \text{ cm}^{-1}$  (OH rocking, twisting, or wagging). It is difficult to assign these

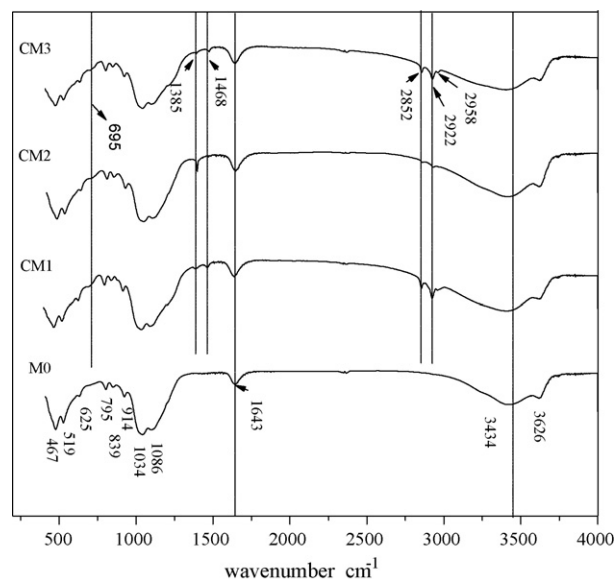


Fig. 2. FTIR spectra of host montmorillonite (M0) and complex modified montmorillonite (CM1, CM2, and CM3).

**Table 1**  
Infrared frequencies and assignment of montmorillonite.

Position/cm <sup>-1</sup>	Assignments	Position/cm <sup>-1</sup>	Assignments
3626	OH stretching of structural hydroxyl groups	839	Al–Mg–OH deformation
3434	OH stretching of water	1034	Si–O stretching
2958	Symmetric stretching of the CH <sub>3</sub>	914	Al–Al–OH deformation
2922	CH <sub>2</sub> antisymmetric stretching	795	Si–O stretching of cristobalite
2852	CH <sub>2</sub> symmetric stretching	695	Si–O stretching of quartz
1643	OH deformation of water	624	Coupled Al–O and Si–O, out of plane
1468	CH <sub>2</sub> bending	519	Al–O–Si deformation
1385	NO <sub>3</sub> stretching	467	Si–O–Fe deformation
1086	Si–O stretching of cristobalite		

**Table 2**  
The surface and size characteristics of host montmorillonite (M0) and complex modified montmorillonite (CM1, CM2, and CM3).

Species	Surface area (m <sup>2</sup> /g)	Mesoporous volume (cm <sup>3</sup> /g)	Average mesoporous diameter (nm)	Microporous volume (cm <sup>3</sup> /g)
M0	73.2	0.153	7.81	0.0170
CM1	114.0	0.125	4.46	0.0288
CM2	117.2	0.129	4.39	0.0292
CM3	115.8	0.139	5.08	0.0303

bands more precisely. Indeed, the 695 cm<sup>-1</sup> band position is almost certainly influenced by the presence of surrounding Fe ions. The modified montmorillonite samples exhibit broader bands near 3434 cm<sup>-1</sup> and a shift at lower frequencies, which can be attributed to an OH stretching either from water or from the protonated ligand. The assignments are based on previous reports of montmorillonite and polyoxometalates samples [44]. As shown in Fig. 2, a vibration mode at 1385 cm<sup>-1</sup>, attributed to the NO<sub>3</sub> stretching mode, was observed in the FTIR spectra of modified clays. It has been reported that the NO<sub>3</sub> band suggests that some redundant positively charged iron species outside the interlayer of montmorillonite might exist, and act as counterions to balance the positive charge of the iron species [44]. Shoulders characteristic of symmetric stretching of the CH<sub>3</sub> groups on the alkyl chains at 2958 cm<sup>-1</sup> and bands due to the CH<sub>2</sub> groups of the alkyl chains at 2922 cm<sup>-1</sup> and 2852 cm<sup>-1</sup> (antisymmetric and symmetric stretching), 1468 cm<sup>-1</sup> (bending) are present for modified montmorillonites. All of these demonstrate the existence of –CH<sub>n</sub> and can be evidences for binding of the polar segment of the surfactant, which are consistent with literature data [45].

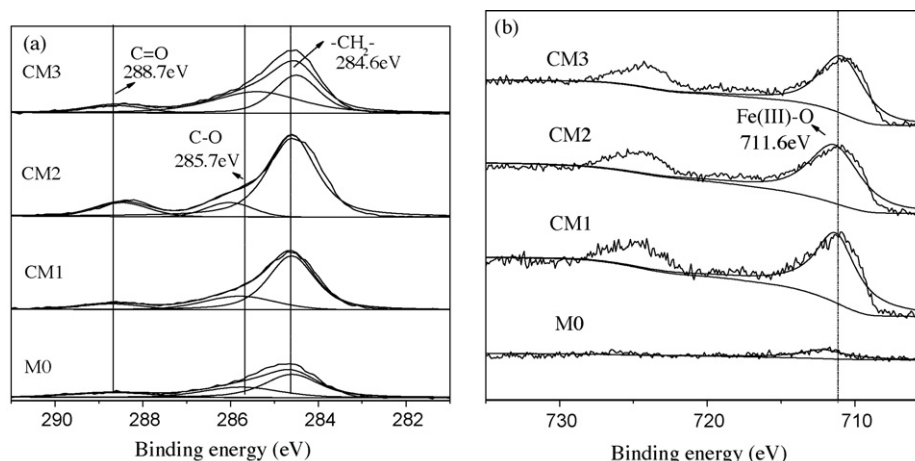
### 3.1.2. XPS experiments

In order to observe the existence of Fe and its combination with OH more precisely, the XPS spectra of the C 1s and Fe 2p<sub>2/3</sub> levels are shown in Fig. 3(parts a, b). The C 1s and Fe 2p<sub>2/3</sub> main peaks

are at 284.6 eV and 711.6 eV, respectively. These values are consistent with those reported in the literature for Fe(III) and –CH<sub>2</sub>– [46,47]. The high intensity of –CH<sub>2</sub>– and Fe(III)–O contributions from complex modified montmorillonites is attributed to the pillaring process, which is consistent with a high coverage of SDS and Fe(III) oxyhydroxide at the surface. The –CH<sub>2</sub>– component indicates the appearance of SDS. The weak signals of C=O at 288.7 eV and C–O at 285.7 eV may be due to the influence of substances used in the production of the host montmorillonite. From Fig. 3(b), we can see that Fe(III) species are rare in M0. However, they are believed to play a crucial role in adsorption and catalyzing the oxidation process [48]. The spectra of Fe 2p are qualitatively equivalent for each modified montmorillonite, and analysis of these spectra indicates that the modified montmorillonite surface was covered by a Fe(III) oxyhydroxide layer.

### 3.1.3. Size characteristics

The textural properties established from the nitrogen sorption isotherms are indicated in Table 2. The specific surface area of the host montmorillonite is 73.2 m<sup>2</sup>/g, while for the modified montmorillonites it is 117.7 m<sup>2</sup>/g, 114.0 m<sup>2</sup>/g, and 115.8 m<sup>2</sup>/g, respectively. The composites have much higher surface areas but smaller mesopore volumes and average mesoporous diameter than for the host montmorillonite. This confirms that the modified species used during preparation entered between the montmo-

**Fig. 3.** XPS spectra of (a) C 1s, (b) Fe 2p<sub>2/3</sub> in Al K $\alpha$  for host montmorillonite (M0) and complex modified montmorillonite (CM1, CM2, and CM3).

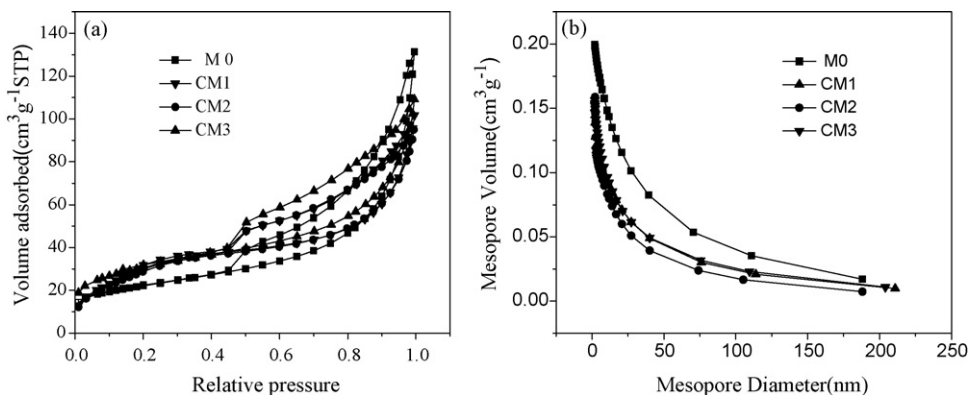


Fig. 4. (a) Nitrogen adsorption–desorption isotherms, (b) BJH pore size distributions of host montmorillonite (M0) and complex modified montmorillonite (CM1, CM2, and CM3).

rillonite layers, increasing nitrogen accessibility. Most research has shown that the total pore volume and average pore diameter changes are mainly related to microporosity, and the pillaring methods result in more micropores [49–51]. Fig. 4, which displays the nitrogen adsorption–desorption isotherms and pore size distributions of the four kinds of montmorillonites, demonstrates that the mesoporous distributions of modified montmorillonites are very similar and the mesopore volumes of the montmorillonites decrease after modification. However, there is an increase in the proportion of smaller diameter pores, especially for the modified montmorillonites. Hence, the decrease in mesoporous volume and mesoporous diameter may be attributed to blockage of some mesopores by the pillaring process, leading to smaller volume and diameter.

### 3.2. Results of the adsorption experiments

#### 3.2.1. Effect of contact time

Adsorption experiments with Cu(II) at pH >6.0, or for Co(II) at pH >8.0 will have precipitation of the metal hydroxide, which introduces uncertainty into the interpretation of the results. The results show that up to pH values of 8–9, the dominant chemical form of Co in aqueous media is Co<sup>2+</sup>. Above pH 9, forms like CoOH<sup>+</sup> and Co(OH)<sub>2</sub>(aq) become increasingly present [52]. Accordingly, it is apparent that, within the experimental conditions of this study, the dominant form of cobalt in aqueous media is Co<sup>2+</sup>. Thus the pH of the solution was adjusted to be acidic. In these experiments, the pH of Cu(II) and Co(II) solutions was adjusted to 5.0 by addition of 0.01 mol/L HCl or NaOH solution. The adsorption results for vari-

ous contact times are shown in Fig. 5. The efficiency of adsorption is high with 30 min enough to almost reach equilibrium and after 45 min equilibrium is achieved. This characteristic is desirable for the treatment of industrial wastewater and for emergency use, e.g. the leakage of contaminated water, metal ions pollution in groundwater, water pollution emergency, which need rapid adsorbents.

#### 3.2.2. Effect of pH

The primary concentration of the Cu(II) and Co(II) solutions was 100 mg/L and 40 mg/L, respectively. The pH of the solution was adjusted to be acidic. Since a 60 min contact time was found to be enough to reach equilibrium, all the samples were shaken 60 min. Fig. 6 shows the trend in the amount of metal ions adsorbed ( $q_e$ ) with respect to pH. It can be seen that the adsorption of metal ions onto complex modified clay has a strong pH-dependent relationship and the uptake of metal ions by modified-clays increases with an increase in pH. CM2 and CM3 have a higher adsorption capacity than the raw montmorillonite when pH >5, but the lower when pH <4. The influence of pH on adsorption may be explained as follows: At very low pH, the number of H<sup>+</sup> ions exceeds that of metal ions by several times and the metal ions cannot compete with H<sup>+</sup> ions for the binding sites on the montmorillonite. The number of negatively charged surface sites increases with pH, so at high pH values, the metal ions are increasingly removed. Of the three kinds of modified montmorillonites, CM2 is the best adsorbent and CM1 the worst. This result indicates that the way of preparation, especially order of addition of reactants has a significant effect on adsorption behavior. The change in the order of addition will probably cause a change in the surface hydrophobicity. CM1 has more hydrophobic surface

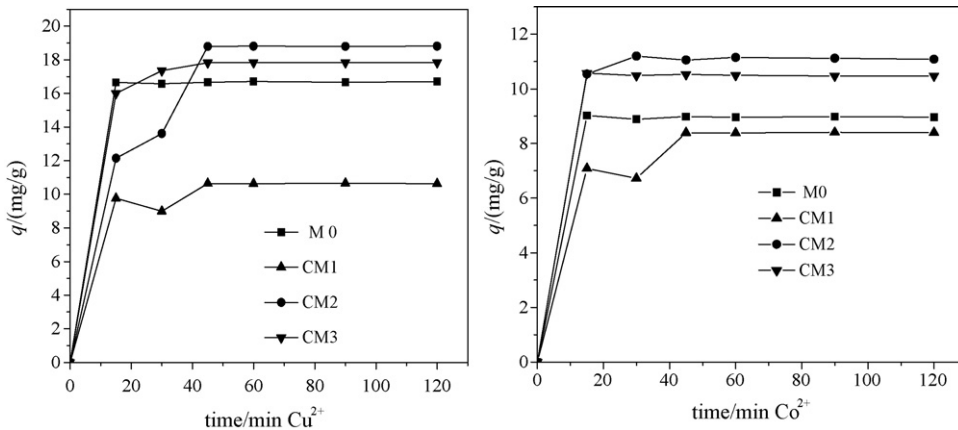


Fig. 5. Effect of time on the adsorption of Cu(II) and Co(II) by host montmorillonite (M0) and complex modified montmorillonite (CM1, CM2, and CM3).

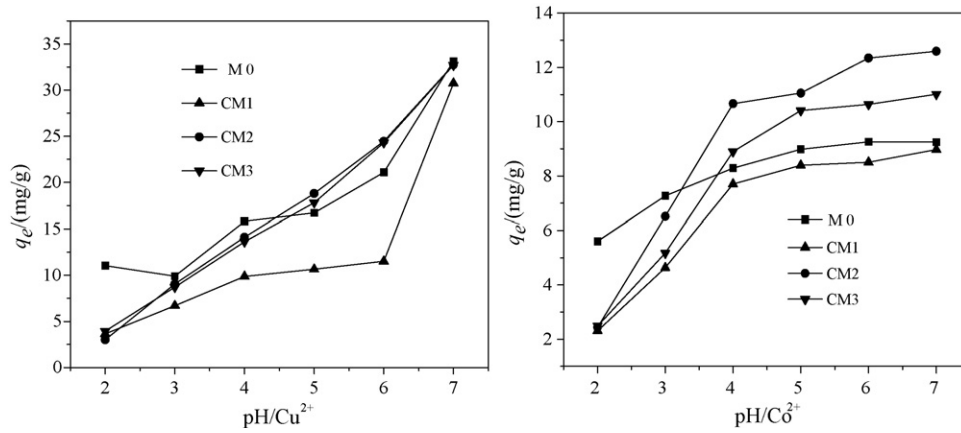
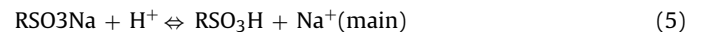
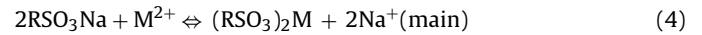


Fig. 6. Effect of pH on the adsorption of Cu(II) and Co(II) by host montmorillonite (M0) and complex modified montmorillonite (CM1, CM2, and CM3).

than other modified clay. The hydrophobic character of CM1, in agreement with some results published earlier, is synthesized using a similar process [7,26–28,33,34]. It is reported that the loading by co-adsorption of surfactant species on pillared montmorillonite increases the affinity of the adsorbent. The surface properties of the adsorbent change from hydrophilic to hydrophobic character and leads to an increasing adsorption capacity for organic compounds. It has also been observed that hydrophobicity is usually related to the change in pH, which affects the solubility or polarity of solutes. The pH of the pillaring solution of CM2 and CM3 is lower than that of CM1 due to the existence of Fe-hydrate solution afterward.

Universally, rules of metal selectivity depend on a number of factors such as the chemical nature of the reactive surface groups, the level of adsorption (i.e. adsorbate/adsorbent ratio), the pH at which adsorption is measured, the ionic strength of the solution and the presence of soluble ligands that could complex the free metal. Fig. 6 shows that the response of  $\text{Co}^{2+}$  to pH is different from  $\text{Cu}^{2+}$  and there are several reasons for it. Specific adsorption plays a more important role than nonspecific adsorption (i.e., cation exchange) of  $\text{Cu}^{2+}$ . Hydroxyl ferrous materials are the most likely to bind Cu in a nonexchangeable form [53]. Cu(II) ions were taken up by the clays as pH was increased with the only limiting factor being the precipitation of Cu(II) as a hydroxide at pH 6.0. The amount of  $\text{Cu}^{2+}$  sorbed is larger than that of  $\text{Co}^{2+}$ , as has been also observed previously [54]. When  $\text{pH} > 6.0$ , the dominating removal process is precipitation and the difference between modified clays and initial clay are not distinct. On the other hand, Co adsorbed by montmorillonite has been identified in two forms. The first form, which is characterized as being slowly dissociable, seems to be bound in a monolayer by chemisorption and would exchange with other  $\text{Co}^{2+}$  ions but

not with a  $\text{Ca}^{2+}$  or  $\text{Mg}^{2+}$  ions. The second form of Co is not dissociable and is believed to either enter the crystal lattice or become occluded in the precipitates of another phase. Otherwise, most clay surface is intercalated with SDS ( $\text{RSO}_3\text{Na}$ ). The exchange reactions in solutions during sorption are shown below [55].



As shown in Eq. (4), the equilibrium constants of  $\text{Cu}^{2+}$  and  $\text{Co}^{2+}$  are different, and this is another reason for the diverse amount of sorption between two metals.

### 3.2.3. Adsorption isotherm

The equilibrium adsorption isotherm data of Cu(II) and Co(II) at varying concentration were analyzed using Freundlich (Eq. (6)) and Langmuir (Eq. (7)) adsorption expressions [53]:

$$q_e = K_F C_e^n \quad (6)$$

$$q_e = b \left( \frac{K_L C_e}{1 + K_L C_e} \right) \quad (7)$$

where  $K_F$  and  $n$  are the Freundlich constants and  $K_L$  is the Langmuir constant. The quantity  $q_e$  of Cu(II) and Co(II) adsorbed is related to the equilibrium solution concentration of the adsorbate  $C_e$  by the parameters  $K_L$  and  $b$ . The steepness of the isotherm is determined by  $K_L$ .  $K_L$  can be looked upon as a measure of the affinity of the adsorbate for the surface.  $b$  is the monolayer capacity and it is commonly

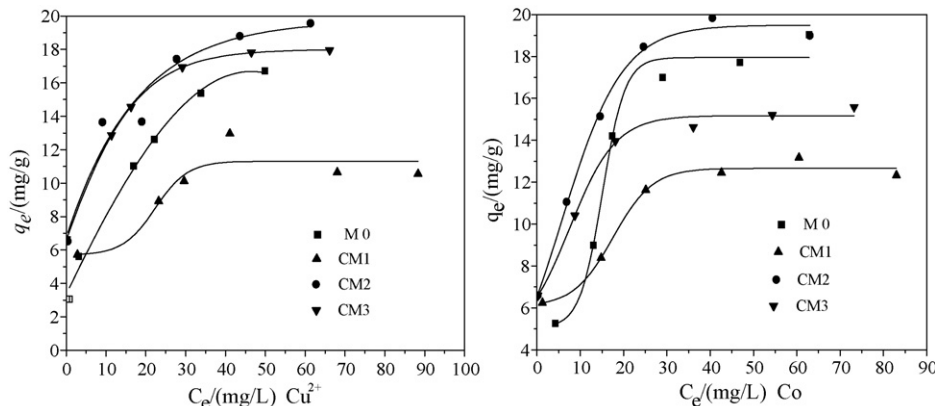


Fig. 7. The Langmuir adsorption isotherms of Cu(II) and Co(II) by host montmorillonite (M0) and complex modified montmorillonite (CM1, CM2, and CM3).

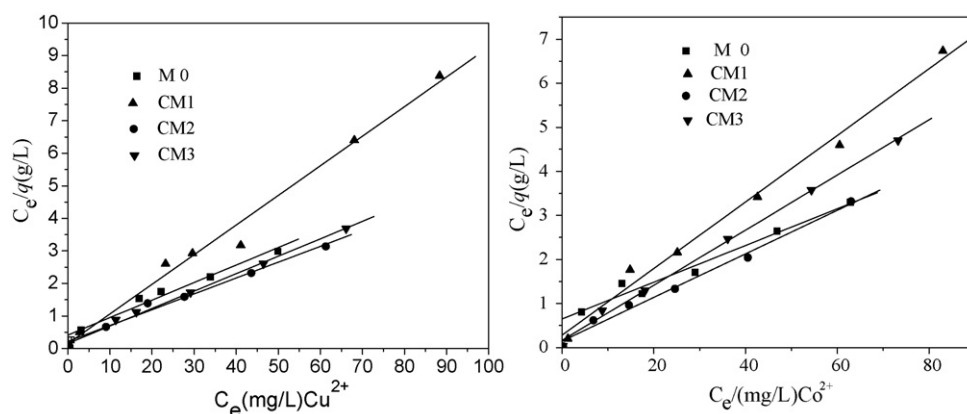


Fig. 8. Linearized Langmuir plot for Cu(II), Co(II) adsorption by host montmorillonite (M0) and complex modified montmorillonite (CM1, CM2, and CM3).

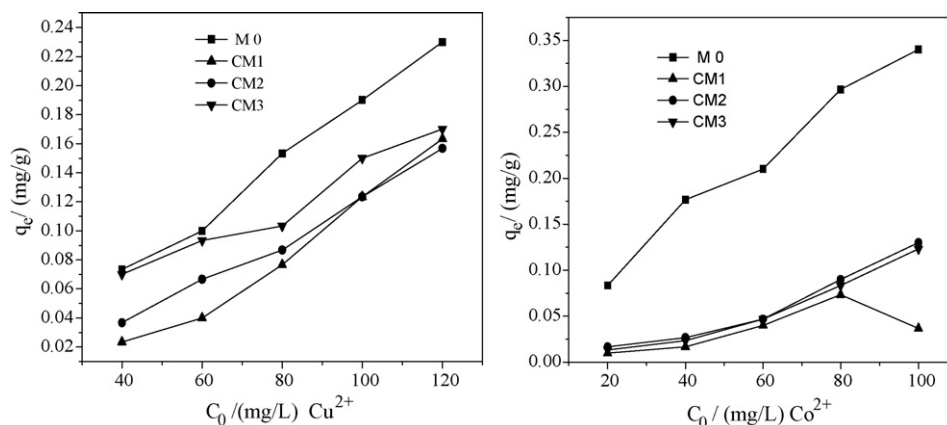


Fig. 9. Desorption plots of Cu(II) and Co(II) from host montmorillonite (M0) and complex modified montmorillonite (CM1, CM2, and CM3).

denoted by the maximum adsorption which is determined by the number of reactive surface adsorption sites. The Freundlich and Langmuir parameters were obtained by nonlinear least-squares regression analysis. The parameters are calculated from adsorption data by converting Eqs. (6) and (7) into the linear form:

$$\log q_e = \log K_F + n \log c_e \quad (8)$$

$$\frac{q_e}{c_e} = bK - Kq_e \quad (9)$$

From the adsorption isotherms at Fig. 7, it can be seen that both CM2 and CM3 have greater uptake of Cu(II) than the host montmorillonite, but CM1 is less. CM2 has greater Co(II) adsorption than the host montmorillonite and the other modified montmorillonites, which may be related to its structure. The linear form of Langmuir isotherm is shown in Fig. 8 and the results of fitting Freundlich and Langmuir equations to isotherm curves are summarized in Table 3. The  $r^2$  (coefficient of determination) of the Langmuir equation and the Freundlich equation is calculated. The  $r^2$  values of the

Langmuir equation are all >0.98, greater than for the empirical Freundlich equation. The value of  $q_i$  is 18.60 mg/g, 20.21 mg/g for M0, and 20.56 mg/g, 20.21 mg/g for CM2 of Cu(II) and Co(II) adsorption, respectively. These values indicate that the Langmuir isotherm is a good fit to the results. CM2 has the best potential to be used as an adsorbent for Cu(II).

#### 3.2.4. Desorption experiment

The intent of the desorption experiment was to determine the ultimate treatment for the adsorbent and to prevent secondary contamination. If the adsorbed metal ions are desorbed easily, the pollutants would be transferred to the desired medium. The initial concentration after the first adsorption, related to the concentration determined by desorption is shown in Fig. 9. There was hardly any desorption of the adsorbents indicating binding sites of the modified montmorillonites are strong.

## 4. Conclusions

The 001 reflection of the host clay was sharper and higher order harmonics appeared, while CM1 and CM3 were dispersed and the intensity was weakened after modification. The results of FTIR reveal that the organic ion has been intercalated into the clay layers. The composites have much greater surface areas but smaller mesopore volumes and average mesoporous diameters than the host montmorillonite. The decrease in mesoporous volume and mesoporous diameter is attributed to blockage of some mesopores by the pillaring process, leading to greater microporous volume and diameter.

Table 3  
Langmuir linearized equations and correlative parameters.

Species	Clays	$q_i$	$b$	$r^2$ (Langmuir)	$r^2$ (Freundlich)
Cu(II)	M0	18.6	0.123	0.988	0.999
	CM1	11.0	0.585	0.992	0.890
	CM2	20.6	0.220	0.992	0.989
	CM3	18.7	0.336	0.997	0.9931
	M0	24.0	0.064	0.987	0.959
Co(II)	CM1	13.2	0.267	0.995	0.954
	CM2	20.2	0.333	0.996	0.976
	CM3	16.0	0.383	0.999	0.984

pH, contact time and metallic concentration can affect the results of adsorption. The optimal pH for modified montmorillonites is 5–6. CM2 is the best adsorbent among the three modified montmorillonites, and CM1 the worst. This is due to the hydrophobic property of CM1. The contact time experiment indicates that the efficiency of adsorption is really high; 30 min being enough to almost reach equilibrium and 45 min is more than adequate. This means the modified clays are excellent for practical applications.

The adsorption isotherm experiment indicates that the Langmuir isotherm is a better fit than the Freundlich. CM2 has the best potential to be used as adsorbent for Cu(II). The results of desorption show that there was hardly any desorption of the adsorbents and the binding sites of the modified montmorillonites are strong.

## Acknowledgements

This work was financially supported by the Program for National Science Foundation of China (Grant No. 40573064, 40973075, 40730741); New Century Excellent Talents Program, Ministry of Education, China (Grant No. NCET-06-0747); Science and Technology Plan of Guangdong Province, China (Grant No. 2006B36601004, 2008B030302036); and the Natural Science Foundation of Guangdong Province, China (Grant No. 06025666, 04020017). The authors thank Jim Irish (College of Environmental Science and Engineering, South China University of Technology) for his editing of the English.

## References

- [1] S. Gier, W.D. Johns, Heavy metal adsorption on micas and clay minerals studied by X-ray photoelectron spectroscopy, *Appl. Clay Sci.* 16 (2000) 289–299.
- [2] A. Bakhti, Z. Derriche, A. Iddou, M. Larid, A study of the factors controlling the adsorption of Cr(III) on modified montmorillonites, *Eur. J. Soil Sci.* 52 (2001) 683–692.
- [3] J. Pires, M.L. Pinto, A. Carvalho, M.B. de Carvalho, Adsorption of volatile organic compounds in pillared clays: estimation of the separation factor by a method derived from the Dubinin–radushkevich equation, *Langmuir* 19 (2003) 7941–7943.
- [4] C. Ooka, H. Yoshida, K. Suzuki, T. Hattori, Highly hydrophobic TiO<sub>2</sub> pillared clay for photocatalytic degradation of organic compounds in water, *Micropor. Mesopor. Mat.* 67 (2004) 143–150.
- [5] P. Malakul, K.R. Srinivasan, H.Y. Wang, Metal adsorption and desorption characteristics of surfactant-modified clay complexes, *Ind. Eng. Chem. Res.* 37 (1998) 4296–4301.
- [6] B.S. Krishna, D.S.R. Murty, B.S. Jai Prakash, Surfactant-modified clay as adsorbent for chromate, *Appl. Clay Sci.* 20 (2001) 65–71.
- [7] O. Bouras, J. Bollinger, M. Baudu, H. Khalaf, Adsorption of diuron and its degradation products from aqueous solution by surfactant-modified pillared clays, *Appl. Clay Sci.* 9 (2007) 1–11.
- [8] G. Fetter, G. Heredia, Synthesis of aluminum-pillared montmorillonites using highly concentrated clay suspensions, *Appl. Catal. A-Gen.* 162 (1997) 41–45.
- [9] S. Moreno, E. Gutierrez, A. Alvarez, N.G. Papayannakos, G. Poncelet, Al-pillared clays: from lab syntheses to pilot scale production characterisation and catalytic properties, *Appl. Catal. A-Gen.* 165 (1997) 103–114.
- [10] L.V. Duong, J.T. Klopogge, R.L. Frost, J.A.R. van Veen, An improved route for the synthesis of Al13-pillared montmorillonite catalysts, *J. Porous Mat.* 14 (2007) 71–79.
- [11] S. Letaief, B. Casal, P. Aranda, M.A. Martín-Luengo, E. Ruiz-Hitzky, An improved route for the synthesis of Al13-pillared montmorillonite catalysts, *Appl. Clay Sci.* 22 (2003) 263–277.
- [12] C. Belver, M.A. Bañares-Muñoz, M.A. Vicente, Fe-saponite pillared and impregnated catalysts I. Preparation and characterization, *Appl. Catal. B-Environ.* 50 (2004) 101–112.
- [13] D. Tabet, M. Saidi, M. Houari, P. Pichat, H. Khalaf, Fe-pillared clay as a Fenton-type heterogeneous catalyst for cinnamic acid degradation, *J. Environ. Manage.* 80 (2006) 342–346.
- [14] J. Barrault, M. Abdellaoui, Catalytic wet peroxide oxidation over mixed (Al–Fe) pillared clays, *Appl. Catal. B-Environ.* 27 (2000) 225–230.
- [15] J. Carriazo, E. Guélou, J. Barrault, J.M. Tatibouet, R. Molina, S. Moreno, Synthesis of pillared clays containing Al, Al–Fe or Al–Ce–Fe from a bentonite: characterization and catalytic activity, *Catal. Today* 107–108 (2005) 126–132.
- [16] C.B. Molina, J.A. Casas, A comparison of Al–Fe and Zr–Fe pillared clays for catalytic wet peroxide oxidation, *Chem. Eng. J.* 118 (2006) 29–35.
- [17] J. Feng, X. Hu, P.L. Yue, H.Y. Zhu, G.Q. Lu, A novel laponite clay-based Fe nanocomposite and its photo-catalytic activity in photo-assisted degradation of Orange II, *Chem. Eng. Sci.* 58 (2003) 679–685.
- [18] Q. Chen, P. Wu, Y. Li, N. Zhu, Z. Dang, Heterogeneous photo-Fenton photodegradation of reactive brilliant orange X-GN over iron-pillared montmorillonite under visible irradiation, *J. Hazard. Mater.* 168 (2009) 901–908.
- [19] P. Wu, W. Wu, S. Li, N. Xing, N. Zhu, P. Li, J. Wu, C. Yang, Z. Dang, Removal of Cd<sup>2+</sup> from aqueous solution by adsorption using Fe-montmorillonite, *J. Hazard. Mater.* 169 (2009) 824–830.
- [20] D. Nguyen-Thanh, K. Block, T.J. Bandosz, Adsorption of hydrogen sulfide on montmorillonites modified with iron, *Chemosphere* 59 (2005) 343–353.
- [21] E. Hackett, E. Manias, E.P. Giannelis, Molecular dynamics simulations of organically modified layered silicates, *J. Chem. Phys.* 108 (1998) 7410–7415.
- [22] V.N. Moraru, Structure formation of alkylammonium montmorillonites in organic media, *Appl. Clay Sci.* 19 (2001) 11–21.
- [23] S.H. Lin, R.S. Juang, Heavy metal removal from water by sorption using surfactant-modified montmorillonite, *J. Hazard. Mater.* 92 (2002) 315–326.
- [24] M. Cruz-Guzmán, R. Celis, M. Carmen Hermosín, J. Cornejo, Adsorption of the herbicide simazine by montmorillonite modified with natural organic cations, *Environ. Sci. Technol.* 38 (2004) 180–186.
- [25] R. Ishii, H. Wada, K. Ooi, A Comparison of supercritical carbon dioxide and organic solvents for the intercalation of 4-phenylazoaniline into a pillared clay mineral, *J. Colloid Interf. Sci.* 254 (2002) 250–256.
- [26] O. Bouras, M. Houari, H. Khalaf, Adsorption of some phenolic derivatives by surfactant treated Al-pillared Algerian bentonite, *Toxicol. Environ. Chem.* 70 (1999) 221–227.
- [27] O. Bouras, M. Houari, H. Khalaf, Using of Surfactant Modified Fe-Pillared Bentonite for the Removal of Pentachlorophenol from Aqueous Stream, *Environ. Technol.* 22 (2001) 69–74.
- [28] H. Khalaf, O. Bouras, V. Perrichon, Synthesis and characterization of Al-pillared and cationic surfactant modified Al-pillared Algerian bentonite, *Microporous Mater.* 8 (1997) 141–150.
- [29] R. Wibulswas, D.A. White, R. Rautiu, Adsorption of phenolic compounds from water by surfactant-modified pillared clays, *Process Saf. Environ. Protect.* 77 (1999) 88–92.
- [30] Y.H. Shen, Removal of phenol from water by adsorption–flocculation using organobentonite, *Water Res.* 36 (2002) 1107–1114.
- [31] J.Q. Jiang, N.J.D. Graham, Enhanced coagulation using Al/Fe(III) coagulants: effect of coagulant chemistry on the removal of colour-causing NOM, *Environ. Technol.* 17 (1996) 937–950.
- [32] J.Q. Jiang, N.J.D. Graham, Preparation and characterization of an optimal polyferric sulphate (PFS) as a coagulant for water treatment, *J. Chem. Technol. Biot.* 73 (1998) 351–385.
- [33] P.X. Wu, Z.W. Liao, H.F. Zhang, J.G. Guo, Adsorption of phenol on inorganic-organic pillared montmorillonite in polluted water, *Environ. Int.* 26 (2001) 401–407.
- [34] J.Q. Jiang, Z.Q. Zeng, Comparison of modified montmorillonite adsorbents Part II: The effects of the type of raw clays and modification conditions on the adsorption performance, *Chemosphere* 53 (2003) 53–62.
- [35] J.M. Hellawell, Toxic substances in rivers and streams, *Environ. Pollut.* 50 (1988) 61–85.
- [36] X.L. Wang, T. Sato, B.S. Xing, S. Tao, Health risks of heavy metals to the general public in Tianjin, China via consumption of vegetables and fish, *Sci. Total Environ.* 350 (2005) 28–37.
- [37] N. Zheng, Q.C. Wang, D.M. Zheng, Health risk of Hg, Pb, Cd, Zn, and Cu to the inhabitants around Huludao Zinc Plant in China via consumption of vegetables, *Sci. Total Environ.* 383 (2007) 81–89.
- [38] J.J. Fu, Q.F. Zhou, J.M. Liu, W. Liu, T. Wang, Q.H. Zhang, G.B. Jiang, High levels of heavy metals in rice (*Oryza sativa* L.) from a typical E-waste recycling area in southeast China and its potential risk to human health, *Chemosphere* 71 (2008) 1269–1275.
- [39] M.L. Huang, S.L. Zhou, B. Sun, Q.B. Zhao, Heavy metals in wheat grain: Assessment of potential health risk for inhabitants in Kunshan, China, *Sci. Total Environ.* 405 (2008) 54–61.
- [40] H. Khalaf, O. Bouras, V. Perrichon, Synthesis and characterization of Al-pillared and cationic surfactant modified Al-pillared Algerian bentonite, *Micropor. Mater.* 8 (1997) 141–150.
- [41] P. Yuan, F. Annabi-Bergaya, Q. Tao, M. Fan, Z. Liu, J. Zhu, H. He, T. Chen, A combined study by XRD, FTIR, TG and HRTEM on the structure of delaminated Fe-intercalated/pillared clay, *J. Colloid Interface Sci.* 324 (2008) 142–149.
- [42] G. Lagaly, S. Ziesmer, Colloid chemistry of clay minerals: the coagulation of montmorillonite dispersions, *Adv. Colloid Interface Sci.* 100–102 (2003) 105–128.
- [43] M.A. Vicente, M.A. Banares-Munoz, M. Suarez, J.M. Pozas, J.d.D. Lopez-Gonzalez, J. Santamaria, A. Jimenez-Lopez, Pillaring of a High Iron Content Saponite with Aluminum Polycations-Surface and Catalytic Properties, *Langmuir* 12 (1996) 5143–5147.
- [44] P. Yuan, H. He, F. Bergaya, D. Wu, Q. Zhou, J. Zhu, Synthesis and characterization of delaminated iron-pillared clay with meso-microporous structure, *Micropor. Mesopor. Mater.* 88 (2006) 8–15.
- [45] L.J. Michot, O. Barres, E.L. Hegg, T.J. Pinnavaia, Intercalation of aluminum (Al<sub>13</sub>) polycations and nonionic surfactants in montmorillonite clay, *Langmuir* 9 (1993) 1794–1800.
- [46] P. Behra, P. Bonnissel-Gissinger, M. Alnot, R. Revel, J.J. Ehrhardt, XPS and XAS Study of the Sorption of Hg (II) onto Pyrite, *Langmuir* 17 (2001) 3970–3979.



- [47] K. Artyushkova, J.E. Fulghum, Identification of chemical components in XPS spectra and images using multivariate statistical analysis methods, *J. Electron Spectroscopy* 121 (2001) 33–55.
- [48] C.O. Moses, J.S. Herman, Pyrite oxidation at circumneutral pH, *Geochim. Cosmochim. Ac.* 55 (1991) 471–482.
- [49] A. Gil, A. D a, M. Montes, D.R. Acosta, Characterization of the microporosity of pillared clays by nitrogen adsorption-application of the Horvath-Kawazoe approach, *J. Mater. Sci.* 29 (1994) 4929–4932.
- [50] J.J. Li, M. Zhen, X.Y. Xu, H. Tian, M.H. Duan, A new and generic preparation method of mesoporous clay composites containing dispersed metal oxide nanoparticles, *Micropor. Mesopor. Mater.* 114 (2008) 214–221.
- [51] L.M. Gand a, R. Tranzo, M.A. Vicente, A. Gil, Non-aggressive pillaring of clays with zirconium acetate Comparison with alumina pillared clays, *Appl. Catal. A-Gen.* 183 (1999) 23–33.
- [52] C.  z m, T. Shahwan, A.E. Eroglu, I. Lieberwirth, T.B. Scott, K.R. Hallam, Application of zero-valent iron nanoparticles for the removal of aqueous  $\text{Co}^{2+}$  ions under various experimental conditions, *Chem. Eng. J.* 144 (2008) 213–220.
- [53] H.B. Bradl, Adsorption of heavy metal ions on soils and soils constituents, *J. Colloid Interface Sci.* 277 (2004) 1–18.
- [54] K.G. Bhattacharyya, S.S. Gupta, Adsorption of a few heavy metals on natural and modified kaolinite and montmorillonite: A review, *Adv. Colloid Interface Sci.* 140 (2008) 114–131.